

# Inositol Hexakisphosphate Kinase-2, a Physiologic Mediator of Cell Death\*

Received for publication, August 17, 2004, and in revised form, November 4, 2004  
Published, JBC Papers in Press, November 8, 2004, DOI 10.1074/jbc.M409416200

Eiichiro Nagata<sup>‡§¶</sup>, Hongbo R. Luo<sup>‡¶</sup>, Adolfo Saiardi<sup>‡</sup>, Byoung-II Bae<sup>‡</sup>, Norihiro Suzuki<sup>§</sup>,  
and Solomon H. Snyder<sup>‡\*\*</sup>

From the <sup>‡</sup>Departments of Neuroscience, Pharmacology and Molecular Sciences, and Psychiatry, School of Medicine, The Johns Hopkins University, Baltimore, Maryland 21205 and the <sup>§</sup>Department of Neurology, Keio University School of Medicine, 35 Shinanomachi, Shinjuku-ku, Tokyo 160-8582, Japan

**Diphosphoinositol pentakisphosphate (InsP7) and bis-diphosphoinositol tetrakisphosphate contain pyrophosphate bonds. InsP7 is formed from inositol hexakisphosphate (InsP6) by a family of three inositol hexakisphosphate kinases (InsP6K). In this study we establish one of the InsP6Ks, InsP6K2, as a physiologic mediator of cell death. Overexpression of wild-type InsP6K2 augments the cytotoxic actions of multiple cell stressors in diverse cell lines, whereas transfection with a dominant negative InsP6K2 decreases cell death. During cell death, InsP6 kinase activity is enhanced, and intracellular InsP7 level is augmented. Deletion of InsP6K2 but not the other forms of InsP6K diminishes cell death, suggesting that InsP6K2 is the major InsP6 kinase involved in cell death. Cytotoxicity is associated with a translocation of InsP6K2 from nuclei to mitochondria, whereas the intracellular localization of the other isoforms of the enzyme does not change. The present study provides compelling evidence that endogenous InsP6K2, by generating InsP7, provides physiologic regulation of the apoptotic process.**

PtdIns(3,4,5)P3 (10) and serve as a phosphate donor to proteins.<sup>2</sup>

The formation of InsP7 and InsP8 is mediated by a family of three inositol hexakisphosphate kinases (InsP6Ks) (11–14). Differential functions of the enzymes are implied by their varying intracellular localizations with InsP6K2 being exclusively nuclear, whereas the other two enzymes are both cytosolic and nuclear (12). A role for InsP6K2 in cell death is suggested by the findings of Lindner and co-workers (15, 16) that deletion of InsP6K2 prevents apoptotic actions of interferon  $\beta$  (15, 16) and  $\gamma$ -irradiation (15, 16) in ovarian carcinoma cells, whereas transfection of InsP6K2 augments cell death, and interferon  $\beta$  treatment leads to enhanced InsP6K2 activity.

In the present study we show that transfection of InsP6K2 in multiple cell lines augments apoptotic actions of several cell stressors, accompanied by major increases in InsP7 formation. Although transfection of all three subtypes of InsP6K increases cell death, deleting InsP6K2, but not InsP6K1 or InsPK3, prevents apoptosis. Additionally, apoptotic stimuli elicit translocation of InsP6K2 from nuclei to damaged mitochondria, whereas no alteration in the intracellular localizations of InsP6K1 or InsP6K3 is demonstrable.

## EXPERIMENTAL PROCEDURES

**Cell Lines and Cell Death Assays**—HeLa cells, PC12 cells, Jurkat T cells, and OVCAR-3 cells were transfected with indicated constructs using a Lipofectamine 2000 transfection kit (Invitrogen) and a protocol provided by the manufacturer (17). We routinely obtained a transfection efficiency of over 70% in these cells. HL-60 cells, a promyelocytic cell line, were cultured in RPMI 1640 medium supplemented with 10% fetal bovine serum and 4 mM glutamine. HL-60 cells could not be transfected by Lipofectamine reagent, and we utilized a newly invented Nucleofection™ system (Amaxa, Inc.) to introduce DNA construct into these cells. We regularly obtained a transfection efficiency of over 50% in HL60 cells. The cells were plated at  $5 \times 10^6$  cells/well in 6-well plastic plates 1 day before the experiment, and cell death was induced by the addition of cisplatin (30  $\mu$ M), staurosporine (1  $\mu$ M), etoposide (25  $\mu$ M), or hydrogen peroxide (750  $\mu$ M) (18). For generating hypoxia condition, the transfected cells were cultured at 37 °C for 20 h in a Gas-Pak anaerobic chamber (BD Biosciences, Cockeysville, MD). In parallel, cells grown for the same duration under normoxic conditions served as controls. Toxicity was assayed 12–14 h after drug exposure by microscopic examination with computer-assisted cell counting. The numbers of total and dead cells were determined by nuclear staining with 100 ng/ml 4',6-diamidino-2-phenylindole and propidium iodide (10  $\mu$ M), respectively. After 10 min of incubation, the cells were examined under a fluorescence microscope (Zeiss) with excitation at 360 nm. Cell death was determined as the ratio of dead-to-total cell number and quantified by counting 1,000 cells. For staining of dead cells by terminal deoxynucleotide transferase dUTP nick end labeling (TUNEL) assay, the cells were fixed in 4% paraformaldehyde/phosphate-buffered saline and then stained using a TUNEL assay kit following protocols provided by the

Inositol phosphates are major intracellular signaling molecules with the best known of these, inositol 1,4,5-trisphosphate, releasing intracellular calcium (1, 2). Inositol pyrophosphates occur physiologically, the most prominent being diphosphoinositol pentakisphosphate (InsP7)<sup>1</sup> and bis-diphosphoinositol tetrakisphosphate (InsP8) (3, 4). Inositol pyrophosphates have been implicated in diverse functions including vesicular trafficking (5–7), DNA recombination and repair (8, 9), and chemotaxis (10). Molecular mechanisms whereby they influence these functions are not well established, although there is evidence that InsP7 can compete for PH domain binding with

\* This work was funded by United States Public Health Service Grant MH-18501 and Research Scientist Grant DA-00074 (to S. H. S.). The costs of publication of this article were defrayed in part by the payment of page charges. This article must therefore be hereby marked "advertisement" in accordance with 18 U.S.C. Section 1734 solely to indicate this fact.

<sup>¶</sup> These authors contributed equally to this work.

<sup>§</sup> Present address: Depts. of Pathology and Laboratory Medicine, Harvard Medical School and Children's Hospital Boston, Karp Bldg. 10214, 300 Longwood Ave., Boston, MA 02115.

\*\* To whom correspondence should be addressed: Tel.: 410-955-3024; Fax: 410-955-3623; E-mail: snyder@bs.jhmi.edu.

<sup>1</sup> The abbreviations used are: InsP7, diphosphoinositol pentakisphosphate; InsP8, bis-diphosphoinositol tetrakisphosphate; InsP6, inositol hexakisphosphate; InsP6K, inositol hexakisphosphate kinase; TUNEL, terminal deoxynucleotide transferase dUTP nick end labeling; HPLC, high pressure liquid chromatography; siRNA, small interfering RNA; MOPS, 4-morpholinepropanesulfonic acid; GFP, green fluorescent protein; PI, propidium iodide; HA, hemagglutinin.

<sup>2</sup> A. Saiardi and S. H. Snyder, unpublished data

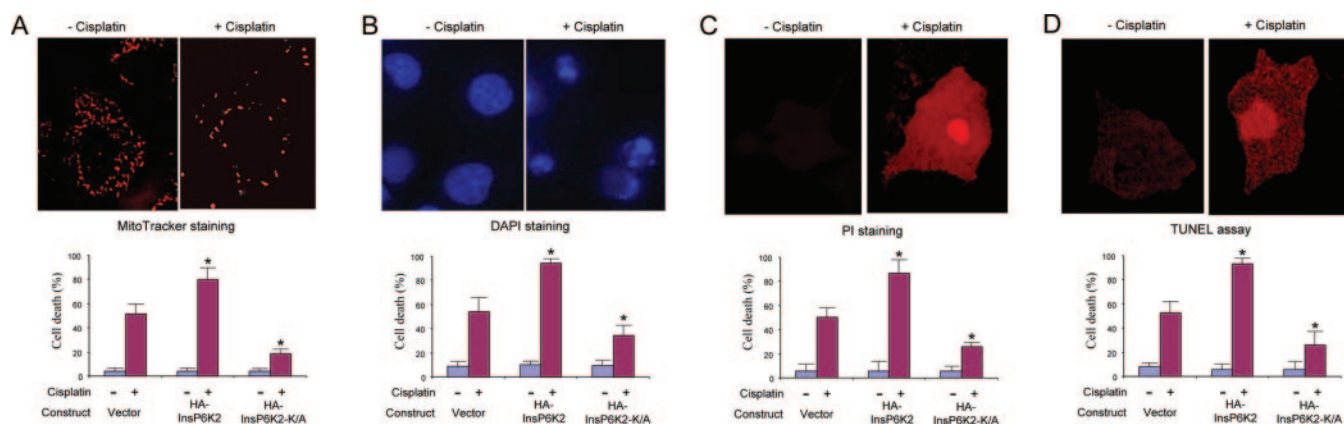


**FIG. 1. InsP6K2 mediates cisplatin-induced apoptosis in NIH-OVCAR-3 cells.** OVCAR-3 cells were cultured in RPMI 1640 medium supplemented with 10% fetal calf serum. The cells were transfected with indicated constructs using a Lipofectamine 2000 transfection kit (Invitrogen) and a protocol provided by the manufacturer. InsP6K2-K/A is a dominant negative InsP2K2. A construct expressing GFP was co-transfected (the ratio between GFP and HA-InsP6K2 constructs is 1:4), permitting monitoring of transfection of IP6K2 gene. Immunostaining with anti-HA antibody confirmed that more than 95% of cells expressing GFP also express HA-tagged fusion proteins (data not shown). The cells were treated with 30  $\mu\text{M}$  anti-cancer drug cisplatin, and toxicity was assayed 14 h after the treatment. In each assay, at least three separate experiments were performed with a minimum of 500 cells counted per data point. Cell death was determined as the ratio of dead-to-total cell number. The results are the means of three independent experiments. The bars indicate the means  $\pm$  S.D. *A*, cell viability assessed by fluorescence microscopy following Mitotracker staining. The cells were incubated with 500 nm Mitotracker Red CMXRos (Molecular Probes) for 20 min. CMXRos is a cell-permeant mitochondrion-selective dye. The uptake of this dye is dependent on mitochondrial membrane potential; therefore the depolarized mitochondria in apoptotic cells will not be stained by CMXRos. For quantitative analysis, a cell was scored as “dead” if less than 100 CMXRos staining positive mitochondria were detected in this cell. *B*, cell viability assessed by fluorescence microscopy following 4',6-diamidino-2-phenylindole (DAPI) nuclear staining. 4',6-Diamidino-2-phenylindole is membrane-permeable and stains both healthy and dead cells. Cells containing obvious condensed nucleus were regarded as “dead” cells. *C*, cell viability assessed by PI staining. PI is membrane impermeable and can only stain the broken (dead) cells. *D*, cell viability determined by the TUNEL assay. Incorporated bromodeoxyuridine into the fragmented DNA was detected using Fluor 488-conjugated anti-bromodeoxyuridine monoclonal antibody. This assay detected fragmented DNA in apoptotic cells.

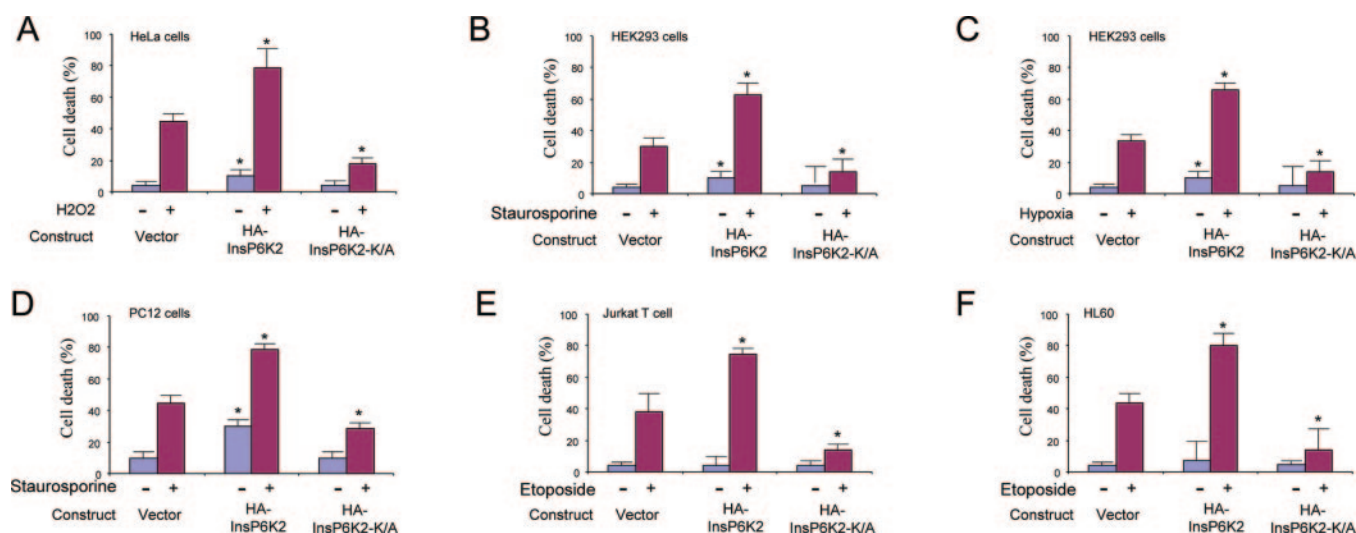


**FIG. 2. InsP6K2 as a mediator of apoptosis in multiple mammalian cancer cell lines.** HeLa, HEK293, PC12, and Jurkat cells were cultured and maintained as previously described (17). These cells were transfected with indicated constructs using the Lipofectamine 2000 reagent (Invitrogen). As in Fig. 1, a construct expressing GFP was co-transfected, permitting monitoring of transfection of InsP6K2 gene. HL-60 cells, a human promyelocytic cell line (28), were cultured in RPMI 1640 medium supplemented with 10% fetal calf serum and 4 mM glutamine. HL-60 cells could not be transfected by Lipofectamine reagent, and we utilized a newly invented Nucleofection™ system (Amaxa, Inc.) to introduce DNA construct into these cells. Nucleofection is an electroporation based technique and uses a combination of special electrical parameters and specific solutions to deliver the DNA directly to the cell nucleus. We regularly obtained a transfection efficiency of over 50% in HL60 cells. Cell death was assessed as described in the legend to Fig. 2. All of these assays provided essentially the same results. The results of PI staining are presented in this figure. *A*, HeLa cells were treated with 750  $\mu\text{M}$  H<sub>2</sub>O<sub>2</sub>, and toxicity was assayed 14 h after the treatment. *B*, HEK293 cells were treated with 1  $\mu\text{M}$  staurosporine, and toxicity was assayed 12 h after the treatment. *C*, HEK293 cells were cultured at 37 °C in a Gas-Pak anaerobic chamber (BD Biosciences). Toxicity was assayed 12 h after the treatment. *D*, PC12 cells were treated with 1  $\mu\text{M}$  staurosporine, and toxicity was assayed 12 h after the treatment. *E*, Jurkat T cells were treated with 25  $\mu\text{M}$  etoposide, and toxicity was assayed 17 h after the treatment. *F*, HL60 cells were treated with 25  $\mu\text{M}$  etoposide, and toxicity was assayed 15 h after the treatment. All of the experiments were repeated for at least three times, and the results are the means of three independent experiments. The bars indicate the means  $\pm$  S.D.

manufacturer (Molecular Probes, Eugene, OR).

**InsP6 Kinase Assay**—Apoptosis of OVCAR-3 cells was initiated by treating cells with 30  $\mu\text{M}$  cisplatin. The cells were lysed at indicated time points, and the resulting lysate was used for activity assay. InsP6 kinase enzymatic activity was assayed as preciously described (11).

**Radiolabeling and Detection of Inositol Phosphates in Intact Cells**—The OVCAR-3 cells were plated at a density of  $0.5 \times 10^6$  cells/35-mm

plate and incubated with [<sup>3</sup>H]inositol (final concentration, 100  $\mu\text{Ci/ml}$ ) for 4 days. The cells were harvested and washed twice with ice-cold DB buffer (10). The cell pellets were lysed in 0.2 ml of ice-cold lysis buffer (2 M perchloric acid, 0.1 mg/ml InsP<sub>6</sub>, 2 mM EDTA). The Lysates were centrifuged for 5 min at 4 °C, and the supernatant was neutralized with K<sub>2</sub>CO<sub>3</sub> as described previously (5). Inositol phosphates were resolved by HPLC as described above.

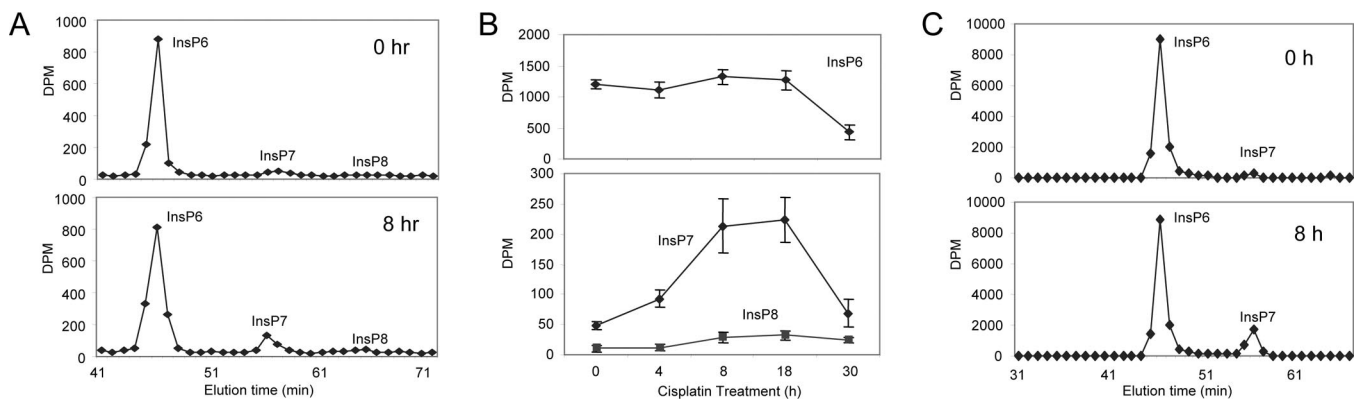


**FIG. 3. InsP7 level is elevated, and InsP6 kinase activity is enhanced during tumor cell apoptosis.** OVCAR-3 cells were plated at a density of  $0.5 \times 10^6$  cells/35-mm plate and incubated with [ $^3$ H] inositol (final concentration, 100  $\mu$ Ci/ml) for 4 days. Apoptosis was initiated by treating cells with 30  $\mu$ M cisplatin. **A**, cells were lysed at indicated time points, and inositol phosphates were extracted and analyzed by HPLC as previously described (6). All of the data were normalized to the total amount of protein extracted from each sample. HPLC profiles at time 0 and 8 h are presented. **B**, the amounts of InsP6, InsP7, and InsP8 in cells were plotted as a function of time after cisplatin challenge. The results are the means ( $\pm$ S.D.) of three independent experiments. **C**, InsP6 kinase activities in apoptosis. At the indicated time points after cisplatin treatment, the cells were collected, and a 30- $\mu$ l cell pellet was resuspended in 10  $\mu$ l of reaction buffer (phosphate-buffered saline containing 20 nM [ $^3$ H]InsP6 and 5  $\mu$ M cold InsP6). Kinase reactions were initiated by filter lysing cells through two layers of 5- $\mu$ m filter. The samples were incubated at 37  $^{\circ}$ C for 10 min, and the reactions were terminated by the addition of 10  $\mu$ l of 1 M HCl. InsP6 was separated from InsP7 by HPLC. The data are presented as the mean values from three independent experiments whose results varied less than 5%. The InsP6K2 assays were performed in the presence of saturating substrate and were linear over time (data not shown), so that increases in catalytic activity most likely represent changes in  $V_{max}$ .

**Disruption of InsP6K Expression by RNA Interference**—The double-stranded RNAs used in RNA interference experiment were synthesized using a Silencer<sup>TM</sup> siRNA mixture kit (Ambion, Inc.). The PCR amplification of each target site (InsP6K1, InsP6K2, and InsP6K3) was performed using primers that contained T7 promoter sequences. We used the following sequences: InsP6K1 (5' primer, 5'-TAA TAC GAC TCA CTA TAG GGA TGT GTG TTT GTC AAA CC, and 3' primer, 5'-TAA TAC GAC TCA CTA TAG GGA CAG GCT GGC TTT CTC), InsP6K2 (5' primer, 5'-TAA TAC GAC TCA CTA TAG GGA TGA GCC CAG CCT TCA GGG, and 3' primer, 5'-CTAA TAC GAC TCA CTA TAG GGC GGG AAG TCA GGT TTT CCA), and InsP6K3 (5' primer, 5'-TAA TAC GAC TCA CTA TAG GGC AGA TGC CGG GGA CAT GAG, and 3' primer, 5'-TAA TAC GAC TCA CTA TAG GGC TCC TAA TGA CAG AGA GG). After synthesis of each double-stranded RNA, siRNA were produced using RNase III, and each siRNA was transfected into HEK293 cells using siPORT<sup>TM</sup> XP-1 transfection agent (Ambion, Inc.). For Northern blotting analysis, total RNAs from cells transfected with InsP6K1, InsP6K2, and InsP6K3 siRNAs were extracted by TRIzol (Invitrogen) and prepared using LiCl precipitation methods. RNA (30  $\mu$ g) was loaded on 1% agarose/formaldehyde/MOPS gel and transferred to Hybond N+ nylon membrane (Amersham Biosciences). Probes for InsP6K1, InsP6K2, and InsP6K3 and glyceraldehyde-3-phosphate dehydrogenase were labeled with [ $\alpha$ - $^{32}$ P]dCTP using oligonucleotide labeling.

**InsP6K2 Translocation**—HEK293 cells (80% confluent) were transiently transfected with plasmids expressing GFP, GFP-InsP6K1, GFP-InsP6K2, and GFP-InsP6K3. After 48 h, transiently transfected cells were incubated with staurosporine (1  $\mu$ M) (Calbiochem, La Jolla, CA) plus MG132, a proteasome inhibitor from Sigma, for 4 h. The cells were then immediately fixed with 4% paraformaldehyde for 2 h and stained with anti-Bax antibody (DAKO). Images of the fluorescent cells were obtained on an Olympus Fluoview confocal microscope.

## RESULTS

**Overexpression of InsP6K2 Augments Cell Death**—In ovarian carcinoma cells Lindner and co-workers (15, 16) noted that transfection of InsP6K2 stimulates cell death elicited by interferon  $\beta$  (15, 16) and  $\gamma$ -irradiation (15, 16). We have extended these findings to multiple cell lines and apoptotic stimuli (Figs. 1 and 2). In ovarian carcinoma cells treated with cisplatin, InsP6K2 transfection augments cell death monitored by Mito-tracker staining for healthy mitochondria, 4',6-diamidino-2-phenylindole staining for nuclear structure, propidium iodide (PI) staining for membrane structure, and TUNEL staining for DNA fragmentation (Fig. 1). With all assays InsP6K2 transfection increases cell death by about 50%. To ascertain whether endogenous InsP6K2 mediates apoptotic actions of cisplatin, we transfected cells with kinase-dead InsP6K2, which mark-

edly reduces cisplatin-induced cell death, consistent with a physiologic role for endogenous InsP6K2 in regulating apoptosis. InsP6K2 transfection fails to influence the modest basal level of cell death in untreated ovarian carcinoma cells.

To assess the generality of the role of InsP6K2 in apoptosis, we examined five additional cell lines: HEK293 cells, HeLa cells, PC12 cells, Jurkat T cells, and HL60 cells (Fig. 2). We also employed multiple cell stressors including hydrogen peroxide, staurosporine, etoposide, and hypoxic-ischemia (Fig. 2). In all cell lines with all stressors, transfection of InsP6K2 increases apoptosis. By contrast, the kinase-dead InsP6K2 prevents cell death in all instances. This prevention is most marked, about 80%, for Jurkat T and HL60 lymphocyte cell lines treated with etoposide, whereas the least anti-apoptotic actions, about 40%, are in staurosporine-treated PC12 cells.

**Cell Stressors Augment InsP7 Formation, and Deletion of InsP6K2 Selectively Prevents Cell Death**—Lindner and co-workers (15, 16) detected enhanced InsP6K catalytic activity in lysates of ovarian carcinoma cells treated with interferon  $\beta$ . We have explored the influence of cell stressors on inositol pyrophosphate levels and the link of the three InsP6K enzymes to cell death. We monitored inositol pyrophosphate formation in intact ovarian carcinoma cells treated with cisplatin (Fig. 3). Cisplatin elicits a major increase in InsP7 formation with a more modest augmentation of InsP8 generation. Maximal increases in InsP7 levels, about 8-fold, occur at 8 and 18 h. By 30 h, the levels of both InsP7 and InsP6 decrease to base-line values, suggesting that the decline reflects cell death rather than intrinsic regulation of enzyme activity. We also detect an 8-fold increase in InsP7 generation from [ $^3$ H]InsP6 in cell lysates 8 h following cisplatin treatment. The increased InsP6K catalytic activity is the same even with diluted cell lysates (data not shown), indicating that the stimulatory action of cisplatin is not exerted upon some soluble constituent distinct from InsP6K. Western blot analysis fails to reveal altered levels of InsP6K1, InsP6K2, or InsP6K3 following cisplatin treatment (data not shown), implying that the stimulation of enzyme activity reflects a covalent modification of the protein such as phosphorylation. Lindner and co-workers (15, 16) also detected no change in InsP6K2 protein level following interferon  $\beta$  treatment of ovarian carcinoma cells.

To ascertain differential roles of the three InsP6K isoforms,

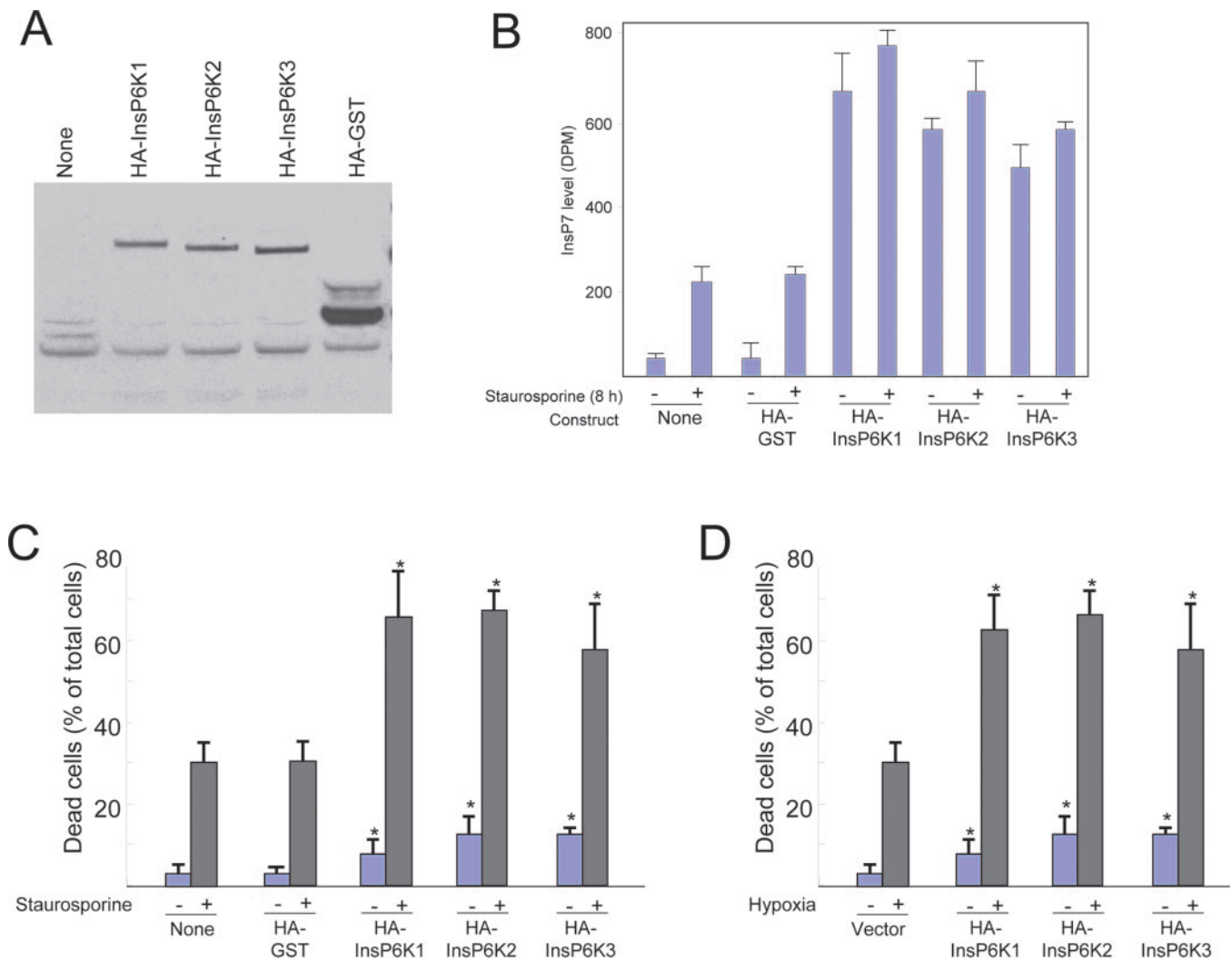


**FIG. 4. Overexpression of InsP6K1 and InsP6K3 also enhances apoptosis.** HEK293 cells were transfected with indicated constructs using the Lipofectamine 2000 reagent. We routinely obtained a transfection efficiency of over 80% using this method. *A*, expression of recombinant proteins was confirmed by Western blotting analysis using an anti-HA antibody. Samples were prepared 24 h after transfection. *B*, the level of InsP7 in transfected cells. The labeling and measurement of intracellular InsP7 was carried out essentially as described in the legend to Fig. 4. The labeling of the cells with [<sup>3</sup>H]inositol started 3 days before transfection and continues thereafter. Apoptosis was triggered by 1  $\mu$ M staurosporine, and inositol phosphates were extracted 8 h after the treatment. Both treated and untreated cells were analyzed. *C*, staurosporine-induced cell death determined by PI staining. Transfected HEK293 cells were treated with 1  $\mu$ M staurosporine, and toxicity was assayed 12 h after the treatment. The transfected cells were identified by co-expression of GFP (see Fig. 2). The results are the means of three independent experiments. The bars indicate the means  $\pm$  S.D. *D*, hypoxia-induced cell death determined by PI staining. The induction of cell death using the Gas-Pak anaerobic chamber was performed as described in the legend to Fig. 3. Toxicity was assayed 12 h after the treatment. The results are the means of three independent experiments. The bars indicate the means  $\pm$  S.D.

we transfected the isoforms and monitored InsP7 formation in intact cells following staurosporine treatment (Fig. 4, *A* and *B*). In untransfected cells staurosporine elicits a 5-fold increase in InsP7 generation. Transfection with each of the three InsP6K isoforms causes a 10–20-fold increase in InsP7 formation with no additional augmentation following staurosporine treatment. The three isoforms are also equally capable of eliciting cell death. Transfection of the three InsP6Ks in untreated cells leads to a 2–4-fold increase in cell death. In staurosporine-treated cells, transfection of the three enzymes doubles the cytotoxic actions of staurosporine. Essentially the same effects are observed with hypoxia treatment.

Although the three forms of InsP6K have the capacity to increase InsP7 formation and augment cell death, transfected proteins do not reflect endogenous conditions. Accordingly, we depleted the three InsP6K isoforms by RNA interference treatment obtaining similar reductions in RNA levels for the three enzymes (Fig. 5). Whereas deletion of InsP6K2 reduces cell death by 60%, deletion of the other two isoforms does not alter

cytotoxicity. Thus, physiologically, InsP6K2 selectively regulates cell viability.

*Cytotoxic Stimuli Cause Translocation of InsP6K2 from Nucleus to Mitochondria*—We wondered whether cell stressors might alter the intracellular localization of InsP6K isoforms and, accordingly, treated HEK293 cells with staurosporine and ovarian carcinoma cells with cisplatin (Fig. 6, *A* and *B*). As reported previously (12), under basal conditions InsP6K2 is almost exclusively nuclear, whereas InsP6K1 and InsP6K3 are both cytosolic and nuclear. The cell stressors do not affect the intracellular localization of InsP6K1 or InsP6K2 but do cause a reduction of nuclear InsP6K2 associated with its appearance in granular structures distributed throughout the cytoplasm.

To ascertain the identity of the granular structures, we looked for possible co-localization of InsP6K2 with targeting sequences for endosomes, endoplasmic reticulum, Golgi, and peroxisomes conjugated with red fluorescent protein. InsP6K2 does not co-localize with any of these markers (data not shown). We evaluated healthy and apoptotic mitochondria stained, re-

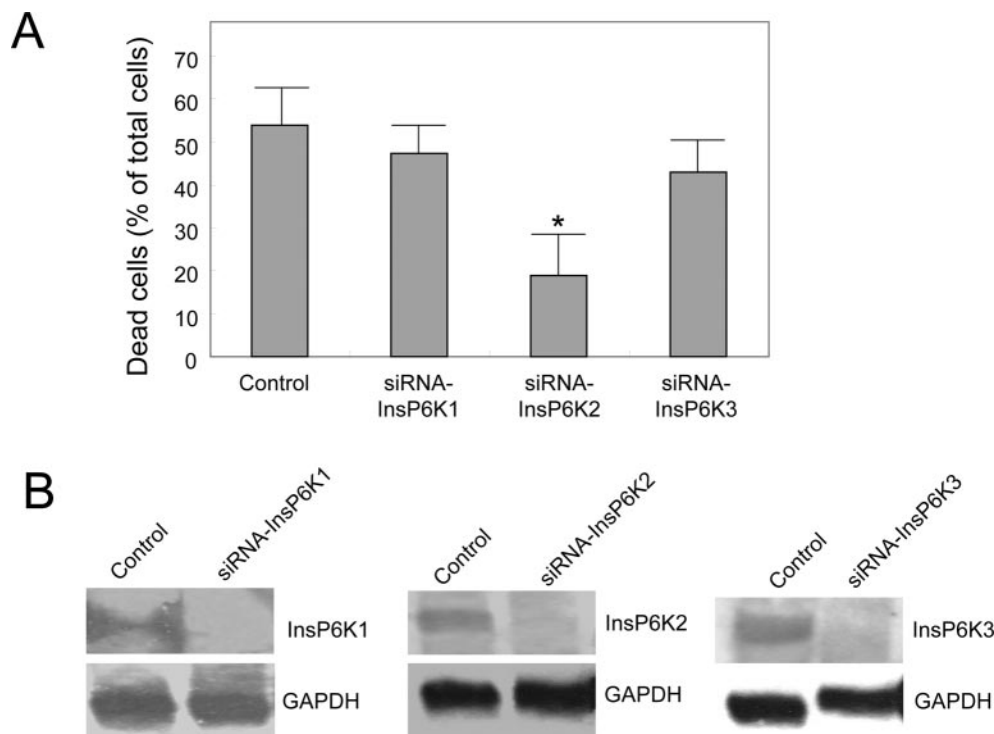


**FIG. 5. siRNA-directed silencing of InsP6K2 gene diminishes staurosporine-induced apoptosis in HEK293 cells.** The siRNAs utilized in this experiment were generated using a Silencer siRNA mixture kit (RNase III) (Ambion) and a protocol provided by the manufacturer. The control is a Negative Control #1 siRNA template provided by the manufacturer. Each siRNA (0.6  $\mu\text{g}/35\text{-mm}$  dish) was transfected into HEK293 cells using siPORT™ XP-1 Transfection Agent (Ambion, Inc.). As in Fig. 1, a construct expressing GFP was co-transfected (the ratio between GFP construct and siRNA is 1:4), permitting monitoring of transfection of InsP6K gene. *A*, HEK293 cells were treated with 1  $\mu\text{M}$  staurosporine, and toxicity was assayed 12 h after the treatment. Cell death was assessed as described in the legend to Fig. 2. All of these assays provided essentially the same results. The results of TUNEL assay are presented in this figure. The results are the means of three independent experiments. The bars indicate the means  $\pm$  S.D. *B*, Northern blot analysis showing reductions in InsP6K1, InsP6K2, and InsP6K3 mRNA levels in cells transfected with siRNAs. The same blot was stripped and reprobated with an anti-glyceraldehyde-3-phosphate dehydrogenase (*GAPDH*) probe as a control for equal sample loading. The Northern blot signals were quantified using NIH Image software. The InsP6K1, InsP6K2, and InsP6K3 mRNA levels were reduced by 90, 75, and 80%, respectively.

spectively, for Mitotracker and Bax (Fig. 6C). Only modest co-localization of InsP6K2 is evident with Mitotracker. By contrast, InsP6K2 co-localizes almost completely with Bax. The selective co-localization of InsP6K2 with Bax, which is well known to translocate from cytosol to mitochondria during apoptosis (19–21), implies an association of InsP6K2 with mitochondria related to the apoptotic process.

#### DISCUSSION

The present study provides compelling evidence that endogenous InsP6K2, by generating InsP7, provides physiologic regulation of the apoptotic process. Thus, multiple cell stressors in diverse cell types all augment InsP7 formation. Deletion of InsP6K2 but not the other forms of InsP6K diminishes cell death. Cytotoxicity is associated with a translocation of InsP6K2 from nuclei to mitochondria, whereas the intracellular localization of the other isoforms of the enzyme does not change.

Transfection of InsP6K2 augments the cytotoxic actions of multiple cell stressors in diverse cell lines, whereas in untreated cells, the transfection increases cell death in some but not other cell lines. We are unable to discern specific factors that explain the differential cytotoxicity of InsP6K2 for various types of untreated cells.

Transfection with kinase-dead InsP6K2 decreases cell death in all cell types examined with different stressors. This finding, similar to what was observed by Lindner and co-workers (15, 16) in a single cell line with a single stressor, evidently reflects a dominant negative action associated with decreased InsP7 formation.

Cell stress leads to an 8-fold increase of InsP7 synthesis, which we detect both in intact cells and in cell lysates with no associated increase in protein levels for any of the three InsP6K isoforms. These observations are best explained by some covalent modification of one of the InsP6K proteins, conceivably by phosphorylation. Alternatively, translocation of InsP6K2 from nuclei to mitochondria may lead to more detectable enzyme activity.

The regulation of apoptosis by InsP6K depends on its catalytic activity. Thus, reducing InsP7 formation by a kinase-dead InsP6K2 diminishes cell death. Moreover, increased generation of InsP7 by transfecting any of the three isoforms augments cell death. Nonetheless, the physiologic regulation of apoptosis appears to selectively involve InsP6K2, because its deletion by RNA interference treatment markedly reduces cell death, whereas deletion of InsP6K1 and InsP6K3 is ineffective. This finding fits with the observations of Lindner and co-workers (15, 16) who first implicated InsP6K2 in this process by showing that InsP6K2 fully accounted for the ability of a library of antisense constructs to reverse cell death elicited by interferon  $\beta$ .

Cytotoxic stimulation elicits a selective translocation of InsP6K2 from nuclei to mitochondria. InsP6K2 co-localizes with mitochondria stained for Bax, reflecting mitochondria damaged during the apoptotic process, but not with Mitotracker, which stains only healthy mitochondria. This finding implies that cell stress causes InsP6K2 to transit from nuclei to mitochondria, where it plays a causal role in initiating the apoptotic process. This possibility is consistent with the ability of InsP6K2 deletion to prevent apoptosis. We do not know what

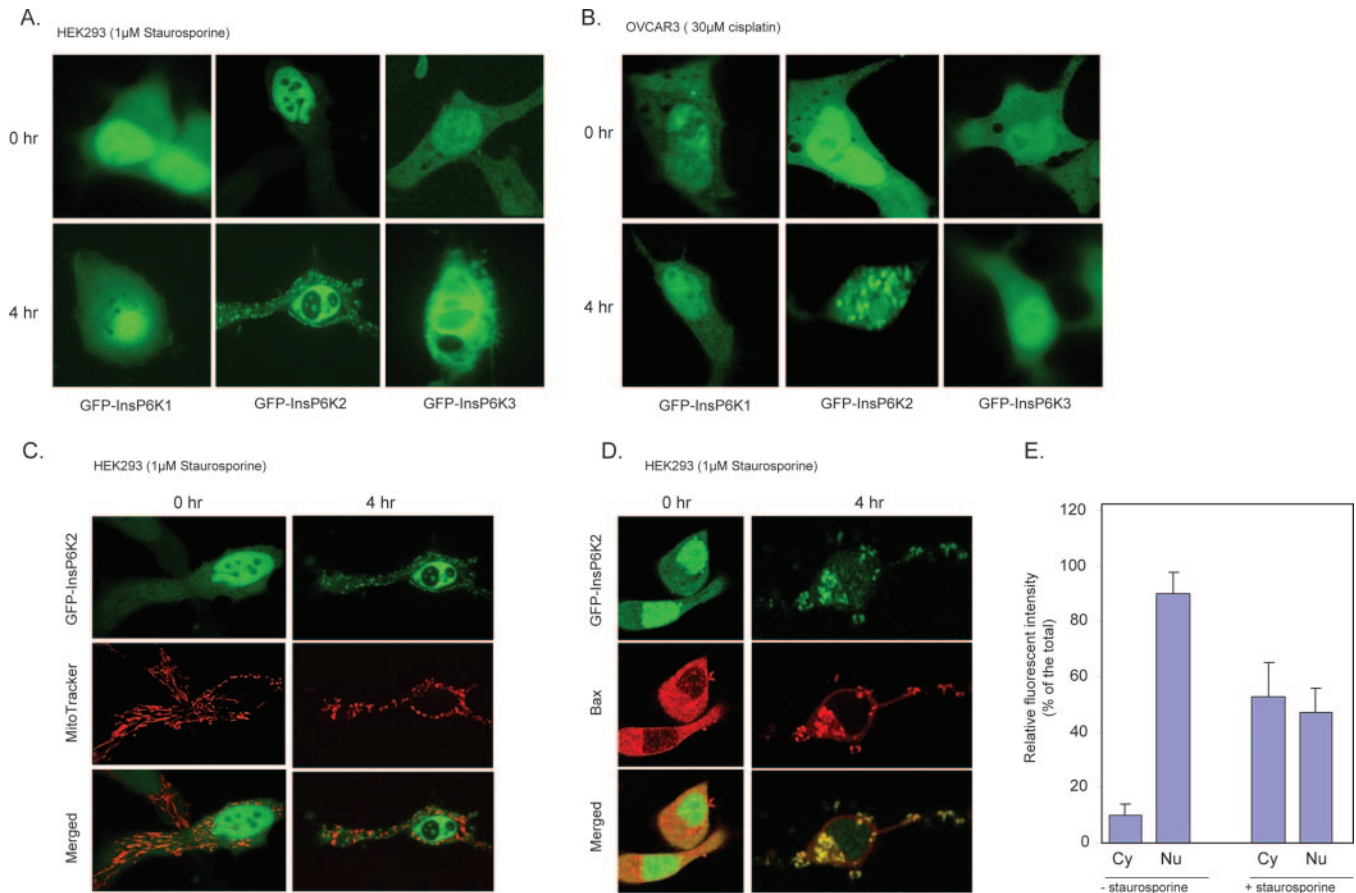


**FIG. 6. InsP6K2 translocates from nucleus to mitochondria during apoptotic cell death.** *A*, InsP6K2 translocation in HEK293 cells treated with staurosporine. HEK293 cells were transfected with indicated constructs expressing InsP6Ks fused with GFP. Transfected HEK293 cells were treated with 1  $\mu$ M staurosporine, and fluorescent images were captured at each of the indicated time points. Each experiment was repeated at least three times, and virtually the same results were obtained each time. The figure shows the results of a representative experiment. *B*, InsP6K2 translocation in OVCAR3 cells treated with cisplatin. OVCAR3 cells were transfected with indicated constructs, and cell death was induced with 30  $\mu$ M cisplatin. Confocal fluorescent images were captured at each of the indicated time points. *C*, InsP6K2 in apoptotic cells does not co-localize with healthy mitochondria. Transfection of HEK293 cells and induction of apoptosis were carried out as described in *A*. Staurosporine-treated HEK293 cells were incubated with 500 nM Mitotracker Red CMXRos (Molecular Probes) for 20 min. The uptake of CMXRos is dependent on mitochondrial membrane potential; therefore only polarized healthy mitochondria can be stained. *D*, InsP6K2 in apoptotic cells co-localizes with depolarized mitochondria. Staurosporine-treated HEK293 cells were immediately fixed with 4% paraformaldehyde for 2 h and immunostained with anti-Bax antibody (DAKO). The images of fluorescent cells were obtained on an Olympus Fluoview confocal microscope. Bax is a marker for depolarized mitochondria (19–21). *E*, quantitative analysis of the cytosolic (Cy) and nuclear (Nu) InsP6K2-GFP. The fluorescence intensities in transfected HEK293 cells were measured with IPLab software as previously described (10). The results are the means of five staurosporine-treated and untreated cells.

accounts for the translocation of InsP6K2 from the nucleus. We have failed to detect any nuclear export signal in InsP6K2. Conceivably cell stress causes a chaperone protein to bind InsP6K2 and move it to mitochondria.

How might InsP7 elicit apoptosis? Known molecular actions of InsP7 include competition with PtdIns(3,4,5)P3 for binding to PH domains of proteins (10) and phosphorylation of proteins.<sup>2</sup> Although InsP7 phosphorylates multiple proteins, only a few have thus far been identified and these are predominantly nuclear.<sup>2</sup> InsP7 competes with phosphatidylinositol 3,4,5-trisphosphate for binding to a variety of PH domain proteins, one of which is Akt (10). By displacing phosphatidylinositol 3,4,5-trisphosphate from Akt, InsP7 diminishes activation of Akt, which is a known survival factor (22–27). This mechanism could explain the pro-apoptotic actions of InsP7.

*Acknowledgments*—We thank all of the members of the Snyder lab for reagents and stimulating discussions.

REFERENCES

1. Berridge, M. J., Lipp, P., and Bootman, M. D. (2000) *Science* **287**, 1604–1605
2. Irvine, R. F., and Schell, M. J. (2001) *Nat. Rev. Mol. Cell. Biol.* **2**, 327–338
3. Glennon, M. C., and Shears, S. B. (1993) *Biochem. J.* **293**, 583–590

4. Stephens, L., Radenberg, T., Thiel, U., Vogel, G., Khoo, K. H., Dell, A., Jackson, T. R., Hawkins, P. T., and Mayr, G. W. (1993) *J. Biol. Chem.* **268**, 4009–4015
5. Saiardi, A., Sciambi, C., McCaffery, J. M., Wendland, B., and Snyder, S. H. (2002) *Proc. Natl. Acad. Sci. U. S. A.* **99**, 14206–14211
6. Luo, H. R., Saiardi, A., Nagata, E., Ye, K., Yu, H., Jung, T. S., Luo, X., Jain, S., Sawa, A., and Snyder, S. H. (2001) *Neuron* **31**, 439–451
7. Ye, W., Ali, N., Bembenek, M. E., Shears, S. B., and Lafer, E. M. (1995) *J. Biol. Chem.* **270**, 1564–1568
8. Huang, K. N., and Symington, L. S. (1995) *Genetics* **141**, 1275–1285
9. Luo, H. R., Saiardi, A., Yu, H., Nagata, E., Ye, K., and Snyder, S. H. (2002) *Biochemistry* **41**, 2509–2515
10. Luo, H. R., Huang, Y. E., Chen, J. C., Saiardi, A., Iijima, M., Ye, K., Huang, Y., Nagata, E., Devreotes, P., and Snyder, S. H. (2003) *Cell* **114**, 559–572
11. Saiardi, A., Erdjument-Bromage, H., Snowman, A. M., Tempst, P., and Snyder, S. H. (1999) *Curr. Biol.* **9**, 1323–1326
12. Saiardi, A., Caffrey, J. J., Snyder, S. H., and Shears, S. B. (2000) *J. Biol. Chem.* **275**, 24686–24692
13. Schell, M. J., Letcher, A. J., Brearley, C. A., Biber, J., Murer, H., and Irvine, R. F. (1999) *FEBS Lett.* **461**, 169–172
14. Saiardi, A., Nagata, E., Luo, H. R., Snowman, A. M., and Snyder, S. H. (2001) *J. Biol. Chem.* **276**, 39179–39185
15. Morrison, B. H., Bauer, J. A., Hu, J., Grane, R. W., Ozdemir, A. M., Chawla-Sarkar, M., Gong, B., Almasan, A., Kalvakolanu, D. V., and Lindner, D. J. (2002) *Oncogene* **21**, 1882–1889
16. Morrison, B. H., Bauer, J. A., Kalvakolanu, D. V., and Lindner, D. J. (2001) *J. Biol. Chem.* **276**, 24965–24970
17. Luo, H. R., Hattori, H., Hossain, M. A., Hester, L., Huang, Y., Lee-Kwon, W., Donowitz, M., Nagata, E., and Snyder, S. H. (2003) *Proc. Natl. Acad. Sci. U. S. A.* **100**, 11712–11717

18. Okuno, S., Shimizu, S., Ito, T., Nomura, M., Hamada, E., Tsujimoto, Y., and Matsuda, H. (1998) *J. Biol. Chem.* **273**, 34272–34277
19. Hsu, Y. T., Wolter, K. G., and Youle, R. J. (1997) *Proc. Natl. Acad. Sci. U. S. A.* **94**, 3668–3672
20. Tsuruta, F., Sunayama, J., Mori, Y., Hattori, S., Shimizu, S., Tsujimoto, Y., Yoshioka, K., Masuyama, N., and Gotoh, Y. (2004) *EMBO J.* **23**, 1889–1899
21. Wolter, K. G., Hsu, Y. T., Smith, C. L., Nechushtan, A., Xi, X. G., and Youle, R. J. (1997) *J. Cell Biol.* **139**, 1281–1292
22. Brazil, D. P., and Hemmings, B. A. (2001) *Trends Biochem. Sci.* **26**, 657–664
23. Downward, J. (1998) *Curr. Opin. Cell Biol.* **10**, 262–267
24. Brunet, A., Datta, S. R., and Greenberg, M. E. (2001) *Curr. Opin. Neurobiol.* **11**, 297–305
25. Cantrell, D. A. (2001) *J. Cell Sci.* **114**, 1439–1445
26. Cantley, L. C. (2002) *Science* **296**, 1655–1657
27. Vivanco, I., and Sawyers, C. L. (2002) *Nat. Rev. Cancer* **2**, 489–501
28. Collins, S. J., Gallo, R. C., and Gallagher, R. E. (1977) *Nature* **270**, 347–349

**Inositol Hexakisphosphate Kinase-2, a Physiologic Mediator of Cell Death**  
Eiichiro Nagata, Hongbo R. Luo, Adolfo Saiardi, Byoung-Il Bae, Norihiro Suzuki and  
Solomon H. Snyder

*J. Biol. Chem.* 2005, 280:1634-1640.

doi: 10.1074/jbc.M409416200 originally published online November 8, 2004

---

Access the most updated version of this article at doi: [10.1074/jbc.M409416200](https://doi.org/10.1074/jbc.M409416200)

Alerts:

- [When this article is cited](#)
- [When a correction for this article is posted](#)

[Click here](#) to choose from all of JBC's e-mail alerts

This article cites 28 references, 15 of which can be accessed free at  
<http://www.jbc.org/content/280/2/1634.full.html#ref-list-1>